

USE OF A NEW REGULATABLE TELOMERASE EXPRESSION SYSTEM TO
MONITOR *IN VITRO* CELL AGING AND THE EFFECTS OF
DNA DAMAGE ON REPLICATIVE SENESENCE

THESIS

Presented to the graduate council
of Texas State University – San Marcos
in Partial Fulfillment
of the Requirements

for the degree

Master of SCIENCE

by

Hiranthi T. Thambugala, B.S.

San Marcos, Texas
August 2005

ACKNOWLEDGEMENTS

The past two years have been the most enlightening and challenging years of my life and I owe it all to you, Dr. Lewis. I truly appreciate everything you have taught me and for your invaluable guidance. You are the most patient, dedicated person and the best mentor and friend any student is lucky to have. I am grateful for the opportunity to have worked with you. Thank you so much.

I would also like to express my thanks to Dr. Jim Irvin and Dr. Rachell Booth for all their advice and help in completing this project. Dr. Booth, it was a pleasure working with you and thank you so much for being so understanding during the stressful times.

To the best set of friends I will treasure my whole life – Brian Wasko, Alison Russell, Sean Schmidt, Jared Cassiano, Shanna Calero, and Vidya Rai. It has been an absolute delight to know each of you and I thank you and wish you all the very best.

I am very grateful to my husband, Chameera, for always believing in me, encouraging me to do my best, and putting up with my chaotic schedule. I love you and I truly appreciate everything you do. Finally, I would also like to thank my family for their support and encouragement.

This manuscript was submitted on July 22, 2005.

TABLE OF CONTENTS

	PAGE
ACKNOWLEDGEMENTS.....	iii
LIST OF TABLES.....	v
LIST OF FIGURES.....	vi
CHAPTER	
I. INTRODUCTION.....	1
II. MATERIALS AND METHODS.....	10
III. RESULTS AND DISCUSSION.....	21
REFERENCES.....	51

LIST OF TABLES

	PAGE
TABLE	
1. Quantitation of the number of viable cells during late senescence of <i>est2⁻</i> cells.....	40

LIST OF FIGURES

FIGURE	PAGE
1. Schematic of telomere replication.....	2
2. Modified DNA bases from oxidative damage.....	6
3. Yeast and human telomerase complexes.....	8
4. Expression vector pLKL82Y.....	22
5. Chromosomal <i>EST2</i> gene disruption via homologous recombination.....	24
6. Model of the <i>EST2</i> expression system.....	25
7. Plate assay of <i>est2</i> ⁻ cells grown on glucose.....	26
8. Liquid growth assay of <i>est2</i> ⁻ cells in glucose.....	28
9. Viability of <i>est2</i> ⁻ cells measured via plating efficiency.....	29
10. Impact of damage-inducing agents on cells.....	30
11. Image of yeast cells at G ₂ checkpoint arrest.....	31
12. Schematic of the cell cycle phases in budding yeast.....	31
13. Quantitation of arrested telomerase-deficient cells in 3% glucose media.....	32
14. Cell density curves and G ₂ /M arrested cell counts of <i>est2</i> ⁻ cells in 5% glucose media	34

15. Cell density curves and G ₂ /M arrested cell counts of <i>est2⁻ rad52⁻</i> in 5% glucose media.....	35
16. Percent viable cell counts of <i>est2⁻</i> cultures in glucose media.	37
17. Percent viable cell counts of <i>est2⁻ rad52⁻</i> cultures grown in galactose or glucose media.....	38
18. Effect of 0.1 µg/ml bleomycin on <i>est2⁻</i> cells.....	42
19. Effect of 0.05 µg/ml bleomycin on <i>est2⁻</i> cells.....	43
20. Streak plate senescence assays of <i>est2⁻</i> and <i>est2⁻ rad52⁻</i> cells	45
21. Streak plate senescence assays of <i>est2⁻</i> and <i>est2⁻ rad52⁻</i> cells exposed to 0.5 µg/ml bleomycin.....	46

CHAPTER I

INTRODUCTION

Eukaryotic chromosome ends consist of thousands of tandem repeats of short GC-rich sequences called telomeres. Telomeres aid in the complete replication of chromosomal DNA and ensure chromosome stability by providing protection against end-to-end fusions, recombination, and degradation. Telomeric DNA along with telomere-specific binding proteins form a “telomere cap”, which provides protection to chromosome ends and regulates its accessibility by telomere processing enzymes. Telomeric repeat DNA differs from the normal chromosomal DNA by its ability to form unique structures such as G-quartets and T-loops. G-quartets exist in two forms - interstrand structures and intrastrand structures - while T-loops are formed by the insertion of the single-stranded 3' overhang of the telomere into the double-stranded DNA thereby distinguishing the ends from double strand breaks that are repaired by the cell.

The major DNA polymerases are unable to synthesize the farthest 5' end of the lagging strand during DNA replication and the absence of such telomeric sequences results in the shortening of chromosomal DNA at both ends with each replication cycle. This “end replicating problem” eventually leads to chromosomal instability as the telomeres shorten and become uncapped (1, 2, 3). To surmount this problem, telomere length is maintained by the enzyme telomerase. Telomerase is a telomere-

specific DNA polymerase, which apart from consisting of protein subunits also consists of an RNA template that dictates the sequence of the added telomeric DNA repeats. Telomeric repeats are added to the 3' end of the telomere using the RNA template by repetitively translocating to the new 3' end of the DNA strand, adding numerous short telomeric sequences during each S phase (Figure 1). Thus, telomerase helps overcome the “end replication problem” brought about by the inability of the major DNA polymerases to completely synthesize the lagging strand during S phase of the cell cycle. The absence of telomerase in cultured human cells causes chromosomes to shorten with every phase of DNA replication eventually leading to cellular senescence (aging) and death.

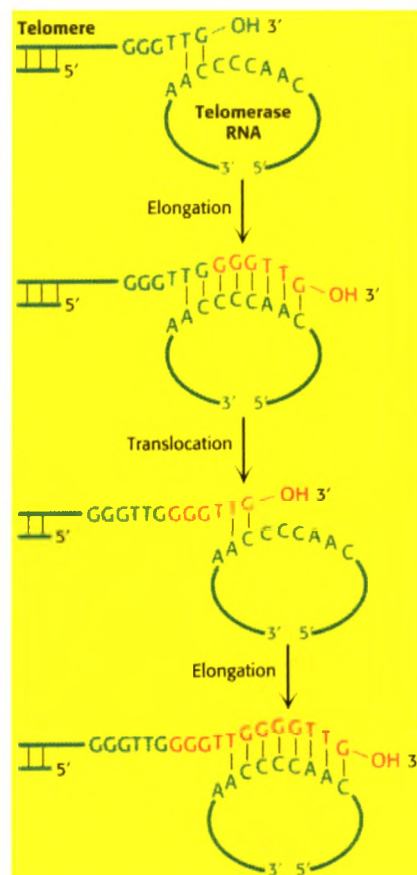


Figure 1. Schematic diagram of telomere replication by telomerase RNA.

In humans the telomeric DNA repeat sequence is TTAGGG. This sequence is repeated more than a thousand times at the ends of each chromosome. Human tissue cells stop producing telomerase shortly after differentiation and thereafter experience a progressive loss of the repeat sequences at the ends of each chromosome. Evidence suggests that shortening may generate “dysfunctional telomeres” leading to chromosome instability. This process has implications for theories of aging, disease susceptibility, and human carcinogenesis (4, 5). For example, telomere length studies conducted on individuals over 60 years old indicated that those with shorter telomeres had a mortality rate that was nearly twice that of those with longer telomeres (6). The Cawthon study also provided evidence that individuals with shorter telomeres had a mortality rate from heart disease that was three-fold higher than those with longer telomeres. The study concluded that older humans of the same age have variable average telomere lengths and that the shorter the telomeres the higher the incidence of death (6). A human genetic disorder, dyskeratosis congenita, arises from insufficient expression of the telomerase RNA gene leading to premature death from bone marrow failure and increased susceptibility to infections, highlighting the importance of telomerase function in dividing human cells (7).

There are two different ways in which the time-dependent shortening of telomeres have been linked with human carcinogenesis. The first model argues that shortening of telomeres, which limits the number of cell divisions, is advantageous in suppressing tumor formation. Cancer cells are immortal, i.e. they grow indefinitely in cell culture, whereas normal primary human cells grown in culture undergo approximately 50 cell divisions (a process termed the Hayflick Limit) and ultimately enter senescence.

Approximately 90% of human cancer cells have reactivated telomerase and have stable chromosome ends (3). Telomerase activity is significantly higher in ovarian cancer cells compared to normal ovarian cells validating the theory that telomerase activation under certain circumstances can be lethal (4, 8). Ongoing research aims at developing anti-cancer therapies that target the synthesis of telomerase (4, 8).

The other model arises from studies indicating that shorter telomeres promote chromosome instability and carcinogenesis. Recent work revealed that an early event in the development of prostate cancer is the formation of shortened, dysfunctional telomeres (5). Increased chromosome instability generated by shortened telomeres is explained by evidence that the ends become uncapped and highly reactive. Furthermore, eventual loss of telomere-associated protein complexes may cause the cell to interpret the broken DNA ends as a form of induced DNA damage and activate checkpoint and/or apoptosis-type responses (9, 10, 11). Other cultured eukaryotic cells such as *Saccharomyces cerevisiae* (budding yeast) cells show similar telomere loss and senescence phenotypes in the absence of telomerase (12), indicating that this is a general phenomenon.

Recent evidence suggests that the rate of telomere shortening in humans and in cultured human cells can be influenced by their cellular environment. Studies conducted by Cawthon *et al.* indicated that women who were under high perceived stress (caregivers) had shorter telomeres that were ten years premature compared to women who had low stress levels (1). These studies are important in understanding factors that promote an early onset of age-related diseases. Another factor that enhances telomere shortening and senescence is oxidative stress. Recent studies provided evidence that reactive oxygen species (ROS), which includes superoxide radicals, peroxy radicals, and

hydroxyl radicals influence aging and age-related diseases (13, 14). The free radicals are produced during normal mitochondrial aerobic respiration and other naturally occurring processes in cells. ROS, particularly hydroxyl radicals, can cause oxidative destruction of biomolecules such as DNA, proteins and lipids. Oxidative damage of nucleic acids gives rise to many DNA lesions, including adducts of base and sugar groups, single- and double-strand breaks, and cross linking to other molecules (14). Some examples of DNA base modifications that arise due to oxidative damage include thymine glycol, N-formamido-urea, 8-oxo-guanine, and 5-hydroxy-methyluracil (Figure 2) (15).

Guanosines within DNA undergo oxidation to produce 8-oxo-2'-deoxyguanosine (8-oxodG), which is utilized as a biomarker for assessing levels of oxidative DNA damage (15, 16, 17). Evidence suggests that the guanine-rich telomeric repeat sequences are also prone to a higher rate of oxidation compared to non-telomeric DNA sequences (16).

Other studies conducted on human fibroblast cells demonstrated that a higher 8-oxodG level exists in senescent cells compared to younger cells and that there is a direct correlation between oxidative DNA damage levels and senescence (13, 17). The pro-oxidants used for these experiments were bleomycin and hydrogen peroxide. Bleomycin, a widely-studied anti-tumor drug, binds iron (Fe) and oxygen to form a free radical complex and causes DNA single- and double-strand breaks (18, 19, 20). Hydrogen peroxide generates peroxy and hydroxyl radicals that cause oxidative damage to biomolecules within cells. Therefore, oxidants appear to play a vital role in the enhancement of telomeric DNA damage, thereby increasing the rate at which telomeres shorten.

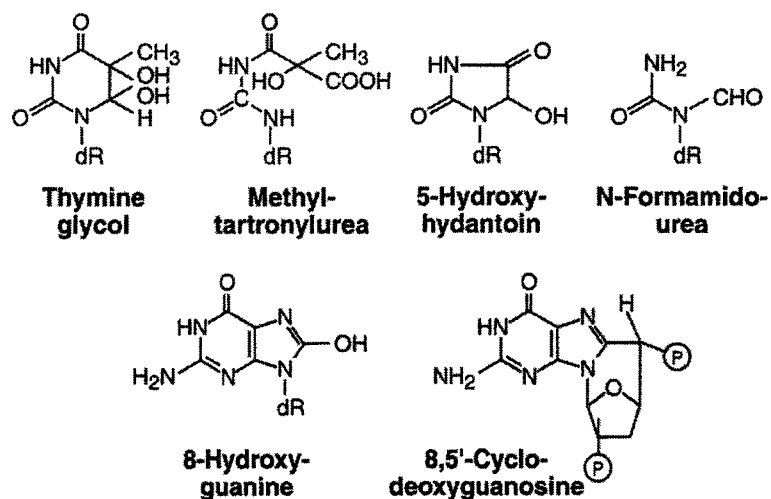


Figure 2. Modified DNA bases resulting from oxidative damage.

To survive in the presence of the oxidants mentioned above and others, cells are equipped with many different types of antioxidant and repair enzymes. Superoxide dismutase (SOD), catalase and glutathione peroxidase (GPX) are examples of antioxidant enzymes. SOD is responsible for the reduction of superoxide anion radicals to molecular oxygen and hydrogen peroxide while both catalase and GPX are involved in the reduction of peroxides (hydrogen peroxide, peroxyxynitrite, etc.) to water or their corresponding hydroxyl compounds (15). Treatment of *Caenorhabditis elegans* (nematode worms) with SOD/catalase mimetics such as EUK-8 (a nonprotein catalytic antioxidant) or EUK-134 (analog of EUK-8 with higher catalase activity) significantly increased their lifespan (21, 22). Isolated rat cardiomyocytes in the presence of EUK-8 were directly protected against oxidative stress (22). Another study exposed transgenic fruitflies, *Drosophila melanogaster*, to SOD and catalase simultaneously. They concluded that there was a significant increase in lifespan and decreased oxidative damage to proteins (23).

In addition to studies proving that oxidants increase the rate of cellular senescence, other studies have investigated the idea that chemical antioxidants that reduce intracellular oxidative damage may delay the onset of senescence. Eukaryotic cells contain many non-enzymatic antioxidants or free radical scavengers – e.g. tocopherols (vitamin E), carotenoids, flavonoids, ubiquinol and ascorbate (vitamin C). Supplementation of human vascular endothelial cells with an oxidation-resistant derivative of ascorbic acid, Asc-2-O-phosphate (Asc2P) reduced the rate at which telomeres shorten by ~52 – 62% thereby extending the cells' lifespans and preventing the enlargement of cell size – a phenotype of senescing cells (24). A striking feature of Asc2P was its ability to increase the amount of intracellular ascorbic acid thereby inhibiting DNA damage brought on by oxidative stress (24). Another study investigated the effect of the spin-trapping agent and lipophilic radical trap, α -phenyl-t-butyl nitron (PBN), an antioxidant, on human diploid fibroblast cells. This antioxidant traps intracellular radical species, forming adducts that keep them from reacting with cellular macromolecules (25). Its elevated distribution within the nucleus and mitochondria and its increased effectiveness in trapping radicals makes it an exceptional antioxidant compared to others (26). Bruce Ames' group demonstrated that the chemical delayed the onset of senescence and extended the replicative life span of human fibroblast cells when compared to other antioxidants such as α -tocopherol, salicylic acid and N-acetylcysteine (17).

Yeast (*Saccharomyces cerevisiae*) and humans have very similar telomerase complexes (Figure 3). The yeast telomerase complex consists of at least five subunits, including the proteins Est1, Est2, Est3 and Cdc13 as well as *TLC1*, the RNA subunit.

Est2 is the catalytic component of the complex. The structure of Est2 resembles a typical reverse transcriptase such as that of the human immunodeficiency virus, which synthesizes DNA from an RNA template (27, 28). Est1 and Cdc13 are single-stranded DNA binding proteins that may target telomerase to 3' overhang structures found at chromosome ends during S phase. *TLC1* RNA contains an internal 17 nucleotide sequence (CACACACCCACACACA) that is used as a template by the enzyme to synthesize new telomeric DNA repeats. Like normal human cells in culture, yeast cells lacking telomerase divide approximately 50-60 times and undergo senescence. Yeast cells that have mutations in the *EST1*, *EST2*, *EST3* or *TLC1* genes exhibit progressive telomere shortening, cellular senescence and eventual cell death (3, 28, 29). A small fraction of cells called “survivors” appear in late passage cultures. These cells have acquired rearrangements and amplified telomere regions resulting in stable telomeres (3). These cells are dependent on the inefficient *RAD52*-mediated homologous recombination process between telomeres. This conclusion comes from the observation that telomerase-deficient cells that lack the essential recombination protein Rad52 do not form survivors (3).

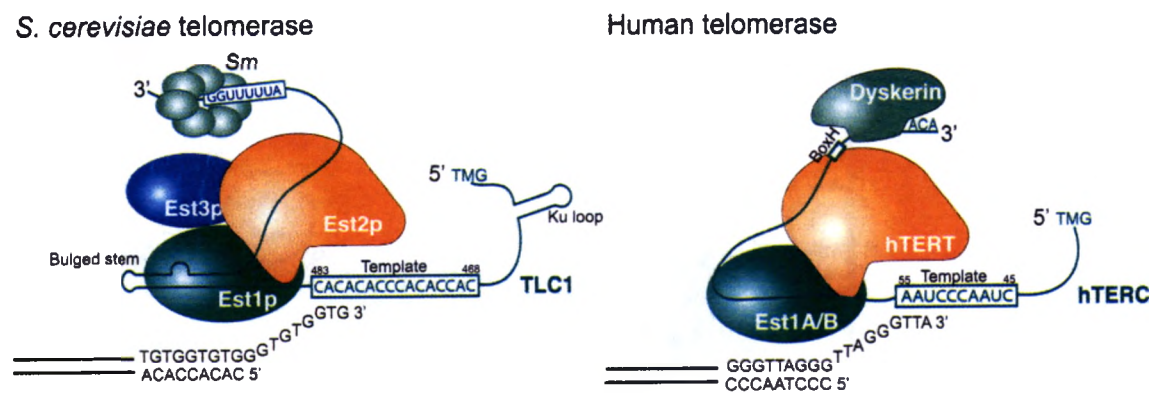


Figure 3. The yeast and human telomerase complexes.

The Lewis lab has recently developed novel galactose-regulated promoters referred to as *GAL1-V4* and *GAL1-V10* that adjoin a polylinker region in new expression vectors (30). These mutant *GAL1* promoters are inducible on galactose media but have low levels of expression when the cells are grown in glucose media. The *GAL1* promoters are positively regulated by the Gal4 activator protein and negatively regulated by the Gal80 repressor protein. When cells are grown in glucose media the Gal80 repressor protein binds to the Gal4 protein preventing the latter from recruiting RNA polymerase to the promoter sequence. Cells in galactose media produce the protein Gal3 which deactivates the Gal80 repressor protein, allowing the Gal4 activator protein to bind to the promoter DNA, thereby facilitating binding of RNA polymerase to the promoter (30, 31, 32).

The primary goals of this research project were to (i) develop and characterize a new system for manipulating senescence by creating an *EST2* polymerase expression vector using the novel *GAL1-V10* promoter described above, and (ii) to investigate the changes occurring as yeast cells age in culture and evaluate the influence of oxidative DNA damage and other types of DNA lesions on the process of senescence.

CHAPTER 2

MATERIALS AND METHODS

I. MATERIALS

General reagents

Ammonium sulfate (granular), sodium chloride and sodium dodecyl sulfate were purchased from Mallinckrodt AR (Paris, Kentucky). Agarose and ethidium bromide were purchased from Shelton Scientific, Incorporated (Shelton, CT). Methyl methanesulfonate (MMS) was obtained from Fluka (Ronkonkoma, NY). Lithium acetate dehydrate, calcium chloride, 99% glycerol, polyethylene glycol (PEG-4000), Sarkosyl (N-lauroyl-sarcosine), Tween 20, magnesium chloride and resveratrol were purchased from Sigma Chemical Company (St. Louis, MO). Sodium acetate was purchased from Mallinckrodt Baker, Inc. (Paris, KY). Tris base was purchased from Invitrogen Life Technologies (Carlsbad, CA). Hygromycin B (HygB), hydrogen peroxide, N-acetylcysteine and bleomycin were purchased from Calbiochem-EMD Biosciences, Inc. (La Jolla, CA). G418 sulfate solution (G418) was purchased from Cellgro-Mediatech, Inc. (Herndon, VA). 5-Fluoroorotic acid (5-FOA) was purchased from US Biological (Swampscott, MA).

Bacteriological and yeast growth media

All amino acids, D-(+)-glucose, and ampicillin were purchased from Sigma Chemical Co. (St Louis, MO). Difco bacto peptone, bacto yeast extract, bacto tryptone and bacto agar were purchased from Becton Dickinson Microbiological Systems (Sparks, MD). Galactose was acquired from Ferro Pfanstiehl Laboratories, Inc. (Waukegan, IL).

Enzymes and PCR reagents

Restriction enzymes were purchased from New England Biolabs (Beverly, MA). Taq Plus Long and PCR reagents were purchased from Stratagene (La Jolla, CA). Ex Taq was purchased from Takara Bio Inc. (Shiga, Japan). T4 DNA Ligase and buffer were purchased from New England Biolabs (Beverly, MA). Shrimp Alkaline Phosphatase was purchased from US Biological (Swampscott, MA).

Cell culture solutions and media

For general, nonselective growth, yeast cells were grown on YPGlu (rich) media (1% bacto yeast extract, 2% bacto peptone, 2% glucose, 2% bacto agar) and/or YPGal media (1% bacto yeast extract, 2% bacto peptone, 2% galactose, 2% bacto agar). In order to assess mitochondrial function, yeast cells were grown on YPG (1% bacto yeast extract, 2% bacto peptone, 2% bacto agar, 3% glycerol). For plasmid selection, yeast cells were grown on synthetic media with drop-out mix (2% glucose or 2% galactose, 2% bacto agar, plus all essential amino acids minus amino acids used for selection). Methyl methanesulfonate (MMS) plates were made using synthetic media or YPGlu plus MMS mixed to obtain various concentrations. HygB and G418 plates were prepared using

YPGlu or YPGal media plus HygB and G418 mixed to 250 $\mu\text{g/ml}$ and 200 $\mu\text{g/ml}$ concentrations, respectively.

Yeast strains

The parent strain used for these studies was BY4742 (*MAT α his3 Δ 1 leu2 Δ 0 lys2 Δ 0 ura3 Δ 0*). The *est2⁻* strain utilized in the assays was YLKL803 (BY4742- *Δ est2 HygB^r* containing plasmid pLKL82Y [*CEN/ARS URA3 GAL1-V10p::EST2*]). YLKL807 was created by inactivating the *RAD52* gene in strain YLKL803 to create a *Δ rad52 G418^r* allele. Diploid cells were made using strains YLKL803 and YLKL817. YLKL817 is YB146 (*MAT α ura3 Δ 52 his3 Δ 200 lys2 Δ 801 trp1 Δ 1 ade2 Δ 101 gal3*), but *Δ est2 .HygB^r* containing plasmid pVL715 [*2 μ URA3 ADH1p::EST2*]. Prior to mating, plasmid pVL715 was removed from YLKL817 by growing cells on 5-FOA plates, which selects against *URA⁺* (plasmid-containing) cells.

II. METHODS

Chromosomal and plasmid DNA purification

For chromosomal DNA, a MasterPure™ Purification Kit by Epicentre Technologies was used following the kit protocol. Plasmid DNA was purified using a rapid boiling lysis method (33).

Yeast transformations

Yeast transformations were performed using either a high efficiency method described by Gietz *et al.* (34) or a rapid DMSO-based transformation method by Soni *et al.* (35).

Construction of pLKL82Y (GAL1-V10p::EST2 URA3) plasmid

PCR of pVL999 (ADH1p::EST2). The *EST2* gene was amplified from the pVL999 plasmid using primers XbaEst2 (TTATTCTAGAGTATTATTAGTACTAATTA ACTA TATG) and BamEst2 (TTATGGATCCATGAAAATCTTATTCGAGTTCATTCAAG) and Taq Plus Long enzyme. The reactions were exposed to the following conditions: 94°C for 2 min., and then 34 cycles (94°C for 30 sec., 48°C for 30 sec., 72°C for 2.5 min.) followed by extension of all unfinished strands at 72°C for 7 min. The PCR samples were run on a 0.7% agarose gel, stained with ethidium bromide and visualized on a Kodak Image Station 440.

Restriction digests of EST2 fragment and pLKL81Y. The *EST2* fragment was digested using *Bam*HI and *Xba*I to generate cohesive ends in the following reaction. In a 1.5 ml microfuge tube the following were added: 8 µl of the *EST2* fragment, 53 µl ddH₂O,

16 μ l 5X KGB buffer, 1 μ l *Bam*HI and 2 μ l *Xba*I. The mixture was incubated at 37°C for 2-4 hours and then precipitated with 2.5 volumes of 100% cold ethanol and resuspended in 8 μ l of TE and 2 μ l of dye-glycerol. A sample of the mixture was run on a 0.6% preparative agarose gel for purification of the cohesive ended *EST2* fragment.

pLKL81Y (*pRS316 GAL1-V10p URA3*) was digested with *Bam*HI and *Xba*I to create a large vector fragment, in the following reaction. In a 1.5 ml microfuge tube, the following were added: 8 μ l pLKL81Y, 37 μ l ddH₂O, 12 μ l 5X KGB, 1 μ l *Bam*HI and 2 μ l *Xba*I. The mixture was incubated at 37°C for 2-4 hours. After incubation, the mixture was treated with shrimp alkaline phosphatase (SAP) to prevent re-ligation of the vector fragment by adding to the reaction: 15 μ l ddH₂O, 4 μ l 5X KGB and 1 μ l SAP. The mixture was incubated at 37°C for 1 hour, and then placed at 70°C for 20 minutes to deactivate the enzymes. A sample was run on a 0.6% preparative agarose gel for purification of the linearized pLKL81Y vector containing the *GAL1-V10* promoter.

Gel purification of GAL1p::EST2 and pLKL81Y vector fragments. Samples of each of the digests were analyzed on a 0.6% preparative agarose gel run in 1X TBE. After briefly visualizing the gel using a UV trans-illuminator, both the large vector fragment and the *EST2* fragment were removed from the gel using sterilized Millipore tweezers. The pieces of gel were placed in a 1.5ml microfuge tube containing a glass wool-packed pipette tip for DNA extraction. The tube was centrifuged at approximately 8,000 x g for 1-2 minutes. The supernatant was transferred to a new microfuge tube and precipitated with sodium acetate and ethanol.

Ligation of EST2 gene fragment and pLKL81Y vector fragment. Each of the purified fragments was quantitated using 2 μ l samples on a Hoefer fluorometer (Hoefer

Pharmacia Biotec Inc., CA). Both fragments were mixed and co-precipitated at a 4:1 molar ratio (insert:vector) in the following reaction mixture: 3.6 μ l (22 ng/ml) *EST2* fragment, 10 μ l (4 ng/ml) pLKL81Y *GAL1-V10* vector fragment, 6.4 μ l ddH₂O, 2 μ l sodium acetate (NaOAc), and 55 μ l 100% ethanol. The mixture was incubated at -20°C for 10 minutes and then centrifuged at full speed for 15 minutes, gently washed with 70% ethanol and respun for 3 min. After discarding the supernatant, the pellet was dried using a Savant Speedvac SC110 and resuspended in the following ligation mixture: 10 μ l ddH₂O, 1.2 μ l 10X T4 ligase buffer, 0.9 μ l T4 DNA ligase. The reaction mixture was incubated at 15°C overnight, transformed into TOP10 *E. coli* cells, and plasmid DNA minipreps were performed on the resulting colonies formed on LB + Amp plates.

Restriction digests of the plasmid DNA minipreps. The plasmid DNA minipreps were digested using *Bam*HI, *Xba*I, *Cla*I, *Afl*III, and *Bgl*II to verify presence and orientation of the *EST2* fragment. Six digest reactions were done (1. *Bam*HI, 2. *Xba*I, 3. *Bam*HI & *Xba*I, 4. *Cla*I & *Xba*I, 5. *Cla*I & *Afl*III and 6. *Cla*I & *Bgl*II). The standard digest reaction follows. In a 0.6 ml microfuge tube the following were added: 1 μ l plasmid DNA, 22 μ l ddH₂O, 6 μ l 5X KGB, and 0.8 μ l of each restriction enzyme. Each mixture was incubated for an hour at 37°C and then precipitated with 2.5 volumes of 100% ethanol, centrifuged at full speed for 10 minutes. The supernatant was discarded; the remaining pellet was dried and resuspended in 8 μ l of TE and 2 μ l of dye-glycerol. A sample of the mixture was run on a 0.8% agarose gel and the presence and orientation of the insert fragment was verified and the new plasmid was designated pLKL82Y (*CEN/ARS GAL1-V10p::EST2 URA3*). The plasmids were transformed into BY4742

cells and grown on Glu-Ura plates for 2 days at 30°C. Individual colonies were streak purified.

Production of YLKL803 ($\Delta est2::HygB'$ -BY4742 containing pLKL82Y)

PCR amplification of the HygB' gene. The Hygromycin B resistance gene (*HygB'*) was amplified via PCR from pAG32 DNA (36) using gESTa2 (CTCATGAAAA TCTTATTCGAGTTCATTCAAGACAAGCTTGACATTGATCTACAG ATGTGACTG TCGCCCGTACATT) and gEST2b2 (TCCTTATCAGCATCATAAGCTGTCAGTATTT CATGTATTATTAGTACTAATTAACGACAAGTTCTTGAAAACAAGAATC) primers and Taq Plus Maxx enzyme. The reactions were exposed to the following conditions: 94°C for 2 min., and then 34 cycles (94°C for 20 sec., 48°C for 30 sec., 72°C for 1.75 minutes) followed by extension of all unfinished strands at 72°C for 7 min. The PCR samples were analyzed on a 0.7% agarose gel.

After transforming BY4742 cells with pLKL82Y, the *HygB'* PCR fragment was transformed into the cells via the high efficiency protocol. Transformants were grown on YPGlu at 30°C for 1 day and then replica-plated onto YPGal + HygB and incubated for 2 days. Individual colonies were patch-purified on YPGlu + HygB, YPGal + HygB and Gal-Ura plates to verify *EST2* gene deletion and plasmid retention.

Confirmation of EST2 gene deletion. The *EST2* gene deletion was confirmed by purifying genomic DNA from individual colonies and doing PCR using test primers 5'EST2 (GAGCTATTGGTGATTTCGCATTTAGGA) and 3'EST2 (GGGAGGCTTTGA AGAAGTAGAAAGGA) and Taq Plus Long enzyme. The reactions were exposed to the following conditions: 94°C for 2 min., and then 34 cycles (94°C for 20 sec., 48°C for 30

sec., 72°C for 2 min 15 sec) followed by extension of all unfinished strands at 72°C for 7 min. The PCR samples were analyzed by gel electrophoresis.

Production of YLKL807 ($\Delta est2::HygB^r \Delta rad52::G418^r$ -BY4742 double mutants containing pLKL82Y)

The G418 resistance gene ($G418^r$) was PCR amplified from the pFA6MX4 plasmid using the gRAD52a2 and gRAD52b2 primers. Samples were run on a 0.7% agarose gel, stained with ethidium bromide and visualized. The $G418^r$ gene fragment was transformed into $\Delta est2::HygB^r$ -BY4742 cells containing pLKL82Y (strain YLKL803). The mixture was grown on YPGlu at 30°C for 1 day. The transformants were replica-plated to YPGlu + G418 and YPGal + G418 and incubated at 30°C for 2-3 days. Individual colonies were patch-purified on YPGal + G418 and incubated at 30°C for 2 days. The patches were replica-plated to YPG, Gal-Ura, YPGlu + 1 mM MMS and YPGlu plates. $RAD52$ gene-deleted isolates were confirmed by their G418 resistance, MMS sensitivities and by PCR using 5'RAD52 and 3'RAD52 test primers.

Creation of $est2/est2$ diploid cells

The strains YLKL455 ($MATa$) and YLKL803 ($MAT\alpha$) were used to make diploid cells. The plasmid pVL715 (2 μ origin $LEU2 ADH1p::EST2$) was transformed into YLKL455 and individual transformants were streak-purified on Glu-Ura plates. An $est2::HygB^r$ PCR fragment was transformed into YLKL455 cells containing pVL715 to disrupt the chromosomal copy of the $EST2$ gene. Transformants were grown on YPGlu + HygB at 30°C for 3 days. HygB^r colonies were patched onto Glu-Ura to check for

plasmid retention and analyzed by PCR using 5'EST2 and 3'EST2 test primers to confirm the gene disruption. After streak-purification, the resulting strain (called YLKL817) was subsequently streaked onto 5-FOA plates to remove the pVL715 plasmid, prior to mating it with YLKL803.

Haploid cells (YLKL803 and YLKL817 that had lost pVL715) were patched on YPGlu plates in three rectangular patches one on top of the other. The *MATa* and *MATα* cells were patched on the top and bottom rectangles and both types of cells were patched together in the middle collectively, one patched horizontally and the other vertically. The plate was incubated at 30°C for 1 day to allow time for *MATa* and *MATα* cells to fuse. The three patches were then replica-plated on selective Glu-Leu-Trp-Ura and Gal-Leu-Trp-Ura plates to select for the diploids. The diploid mating test was confirmed by colonies appearing only in the middle patch (*MATa* and *MATα* cells) and no growth occurring in the individual haploid patches.

Solid media-based senescence assays

To test cellular senescence of the *est2⁻* strain, these cells along with wild type control cells were streaked using sterile toothpicks onto synthetic Glu-Ura and Gal-Ura plates (from individual colonies on a freshly streaked Gal-Ura plate). Once the streaked plates had grown up (30°C, 3 days), individual colonies were picked and restreaked onto fresh Gal-Ura or Glu-Ura plates and allowed to grow and incubated at 30°C as before. This process was repeated until senescence (loss of ability to grow) was observed. This usually became visible on the plate after the fourth streak. The cells grew for

approximately 20 generations with each streak. This same procedure was followed to test cellular senescence in *est2⁻rad52⁻* haploid strains and *est2⁻/est2⁻* diploid strains.

Liquid growth potential and cell viability assay

Culture densities of cells were measured initially by growing overnights from individual colonies in 3 ml Gal-Ura media. Twenty-four hours later, each culture was appropriately diluted and sonicated for approximately 6-8 seconds (Sonics VibraCell™ Ultrasonic Processor). Samples were loaded onto a hemacytometer after which cell counts were obtained using a phase contrast microscope (LOMO Comcon Microscope). After calculating the density (cells/ml) of each overnight culture, fresh 5 ml synthetic and/or rich media cultures were inoculated with a low titer of cells (typically in the range of 20,000-50,000 cells per ml) and shaken at 30°C for 24 hours. This process was repeated each day until the cell densities were too low to measure (6-8 days).

Cell viability counts were obtained by making dilutions of the cell cultures and spreading appropriate volumes onto rich (YPGlu and YPGal) or selective (Glu-Ura and Gal-Ura) plates. These spreads were incubated at 30°C for approximately 3 days. Colonies on each plate were counted and plating efficiencies (% viable cells) were calculated. Plating efficiency was defined as the cells per ml determined from plate counts divided by the cells per ml determined microscopically. This process was repeated for the same duration as the liquid growth potential assays.

Cell-cycle stage quantitation

Cell-cycle counts were performed to determine the effects of the senescence conditions used in the above-mentioned assays. Cells undergoing senescence greatly increase in size and most cells activate cell cycle checkpoint responses due to the cells sensing the shortened chromosome ends as broken or damaged DNA. Normally, cells with damaged chromosomes remain in G₂ phase until most of the damage is fixed, but senescent cells become permanently arrested. Aliquots of the daily liquid cultures were appropriately diluted and sonicated. These samples were loaded onto a hemacytometer and cell types were analyzed (sample size = 100) using phase contrast microscopy. Cell cycle stage was quantitated as follows: unbudded cells were classified as being in G₁ phase, cells with small buds were in S phase, and cells with large buds were termed as being in G₂ or M phase [primarily G₂] (37). The large-budded cells were defined microscopically as cells with buds that were greater than 50% of the size of the mother cell.

CHAPTER 3

RESULTS AND DISCUSSION

The ends of eukaryotic chromosomes are protected by specialized structures called telomeres. These short repeated DNA sequences are maintained by the telomere-specific DNA polymerase telomerase. When telomerase is lacking, chromosomes experience progressive shortening at their ends and eventually enter cell senescence (death) (3, 28, 29). Human somatic cells stop producing telomerase after differentiation and thereafter undergo a progressive loss of DNA sequences at the ends of each chromosome (4, 6). Primary cells grown in culture reflect the same changes that take place in cells *in vivo* during the normal human aging process. That is, cells experience telomere shortening and enter replicative senescence. Telomerase-deficient yeast cells (*S. cerevisiae*) tend to exhibit the same characteristics such as telomere shortening and eventual cell senescence in culture, as seen in human cells.

Although it has been hypothesized that telomere shortening (with uncapping of DNA ends) and chromosome instability promote lethal rearrangements, especially end-to-end chromosome fusions (38, 39, 40), the exact cause of cell death during replicative senescence in human and yeast cells is not known. The initial focus of this research project was to investigate the changes occurring as haploid and diploid yeast

cells aged in culture using a new regulatable telomerase expression system. A major goal of these initial experiments was to demonstrate the usefulness of the *EST2* expression system and also look into the possibility of rescuing cells that would normally die in the 50th and 60th generation, by turning telomerase back on. If end-to-end fusions (dicentric chromosomes) or other dicentric rearrangements are the crucial lethal events that lead to cell death, then reactivation of telomerase should not rescue cells. The second part of this study focused on investigating the links between DNA damage, chromosome instability and *in vitro* cellular aging (replicative senescence). Also, experiments were performed to evaluate the influence of oxidative DNA damage-inducing agents (e.g., hydrogen peroxide and bleomycin) and chemical antioxidants (N-acetylcysteine and resveratrol).

As stated above, the preliminary objective of this study was to develop a system that allowed precise modulation of cellular senescence. This was accomplished by creation of the vector, pLKL82Y, shown in Figure 4 and whose construction is explained in Chapter 2.

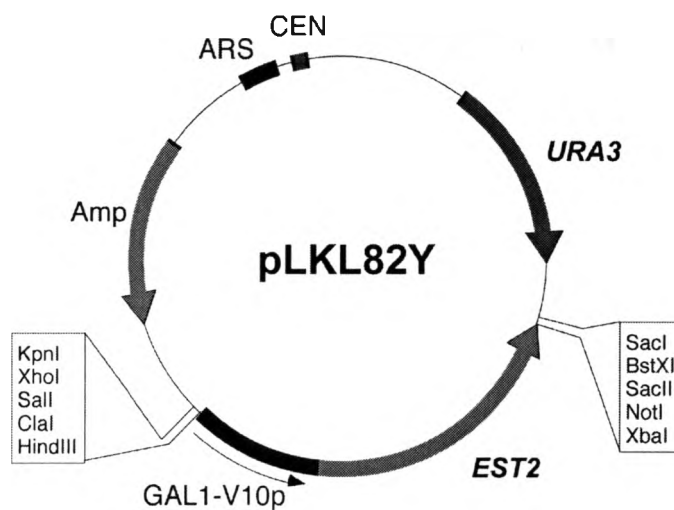
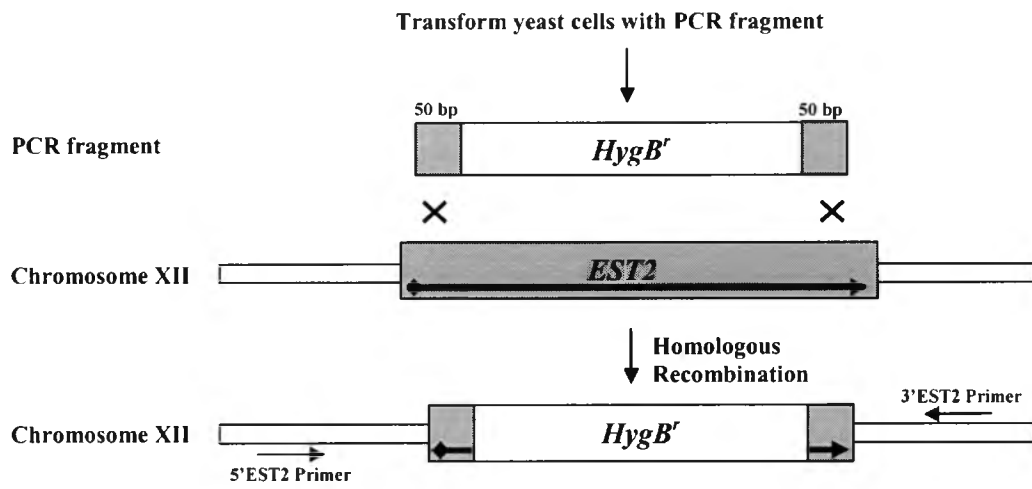


Figure 4. Expression vector pLKL82Y

This shuttle vector has several features, including a centromere resulting in approximately one copy per cell, the *URA3* gene for selection in yeast cells, and the polymerase subunit of yeast telomerase (*EST2*) under the control of a new improved version of the *GAL1* promoter, called *GAL1-V10*. This promoter exhibits very low basal expression when cells are grown in glucose. In contrast, when cells are grown in galactose, this promoter is strongly induced (30).

To construct the system the new plasmid was transformed into BY4742 cells, a common laboratory yeast strain. Then the normal chromosomal *EST2* gene was inactivated as shown in Figure 5A. This gene disruption process involved transformation of cells with a *HygB'* gene PCR fragment (conferring resistance to Hygromycin B) that integrated by homologous recombination into the *EST2* gene locus. Recombination occurred because the PCR fragment contained 50 bp of homology to *EST2* on the 5' end and on the 3' end (Figure 5A). HygB-resistant cells with the correct insertion were confirmed by PCR using the test primers 5'EST2 and 3'EST2 (Figure 5B). The final PCR product if the *HygB'* gene had integrated successfully was approximately 1.5 kb (Figure 5B-Lane 1 and 2). The intact wildtype (wt) *EST2* gene is approximately 2.9 kb (Figure 5B-Lane 3). Therefore in this newly created strain, YLKL803, the only source of Est2 protein is from the plasmid gene.

A



B

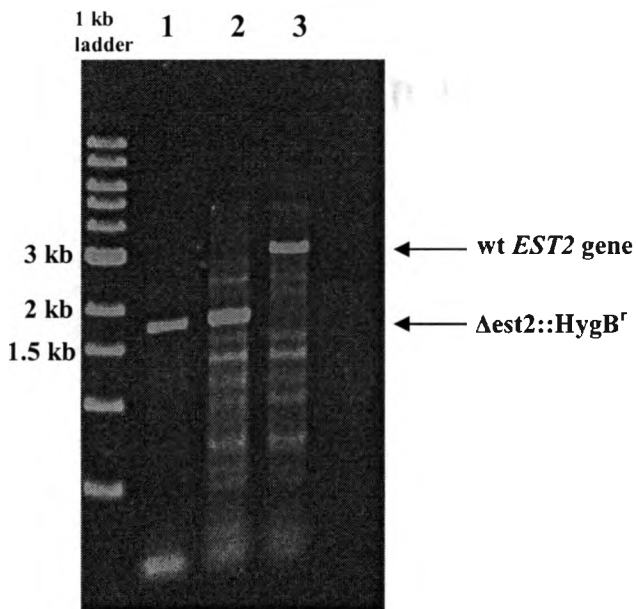


Figure 5. (A) Chromosomal *EST2* gene disruption using homologous recombination.

(B) PCR confirmation of *EST2* gene deletion by verifying the presence of the Hygromycin B resistance gene (*HygB^r*) using test primers 5'EST2 and 3'EST2. (Lane 1 & 2 – *HygB^r+*; Lane 3 – *EST2*⁻)

As shown in Figure 6, when the strain YLKL803 is grown on yeast plates containing galactose, *EST2* is expressed from the plasmid and cells grow normally. However, if cells are grown on glucose plates, *EST2* should not be expressed and cells should undergo senescence (cease to grow after approximately 60 generations). As mentioned previously, in the absence of telomerase the telomeres undergo progressive shortening and cell senescence (Figure 6-right side).

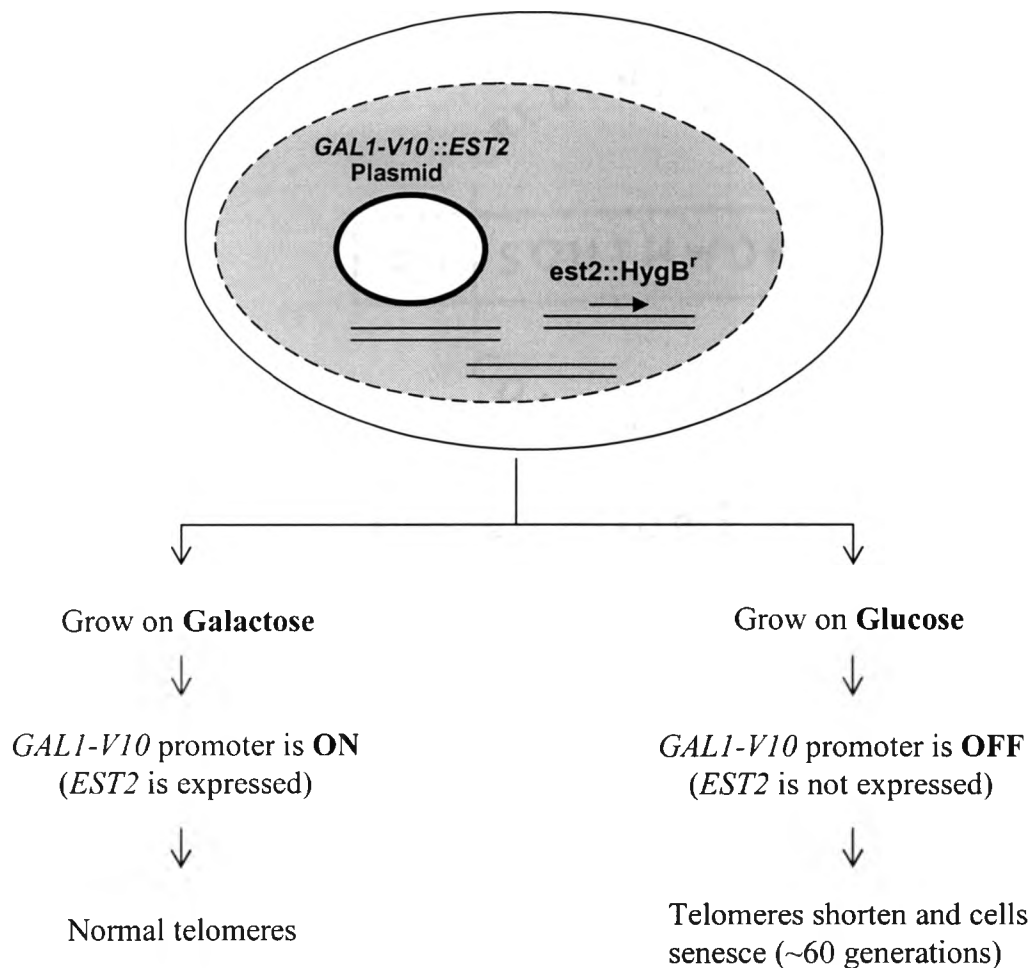


Figure 6. The system created to modulate *EST2* expression and cell senescence.

The new system was initially tested by streaking cells onto glucose plates without uracil (Glu-Ura) and galactose plates without uracil (Gal-Ura), grown for 3 days and restreaked from individual colonies to new plates. After each streak, growing cells divide approximately 20 times and form colonies (Figure 7). The cells grown on glucose (*EST2* not expressed) formed colonies during each of the first three streaks, but did not form normal colonies on the fourth streak plate (after ≥ 60 generations) (Figure 7-left side). In contrast, normal BY4742 cells (telomerase-proficient) continued forming colonies (Figure 7-right side). In both plate and liquid assays (described next) where cells contained the *GAL1-V10::EST2* expression system and were grown on galactose (inducing *EST2* expression), the cells did not undergo senescence.

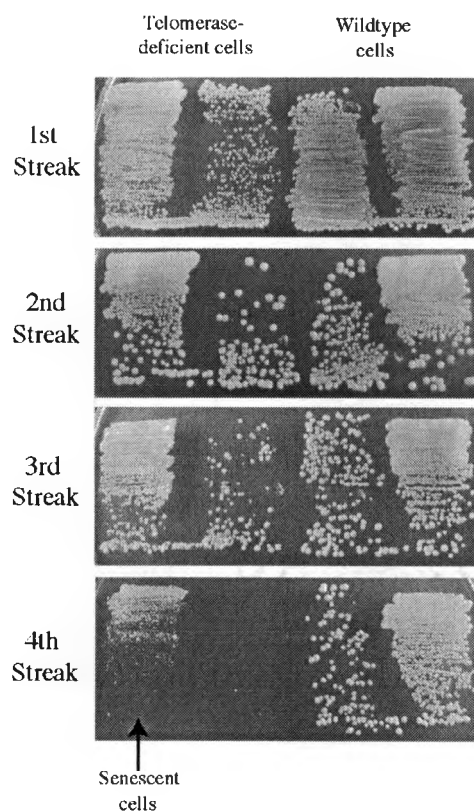


Figure 7. Wildtype BY4742 cells and mutant *est2⁻* cells that contain the *GAL1-V10p::EST2* fusion grown on Glu-Ura plates. The mutant cells exhibit senescence in the 4th streak.

The new system was also tested in liquid growth assays using glucose or galactose media. This liquid-based assay system enabled the quantitative measurement of cell senescence. Cells were harvested and re-inoculated (passaged) daily into liquid 3% glucose (w/v – all sugar concentrations are in this unit of measurement) (Figure 8A). The cells grew at a rate of ~10 – 11 generations per day for 4 to 5 days after which they began to exhibit senescence, that is, slower growth (Figure 8B) in which cells could not reach the same density as on previous days. In contrast, cells propagated in 3% galactose media showed a consistent growth pattern throughout the seven days (Figure 8B). Results were similar using (synthetic) selective growth media or using rich nonselective YP growth media (Figure 8B). Both synthetic and rich (YP) yeast growth media were tested to determine if senescence kinetics was altered when cells grew at different rates. These experiments revealed that loss of growth consistently occurred more rapidly when cells were grown in rich media.

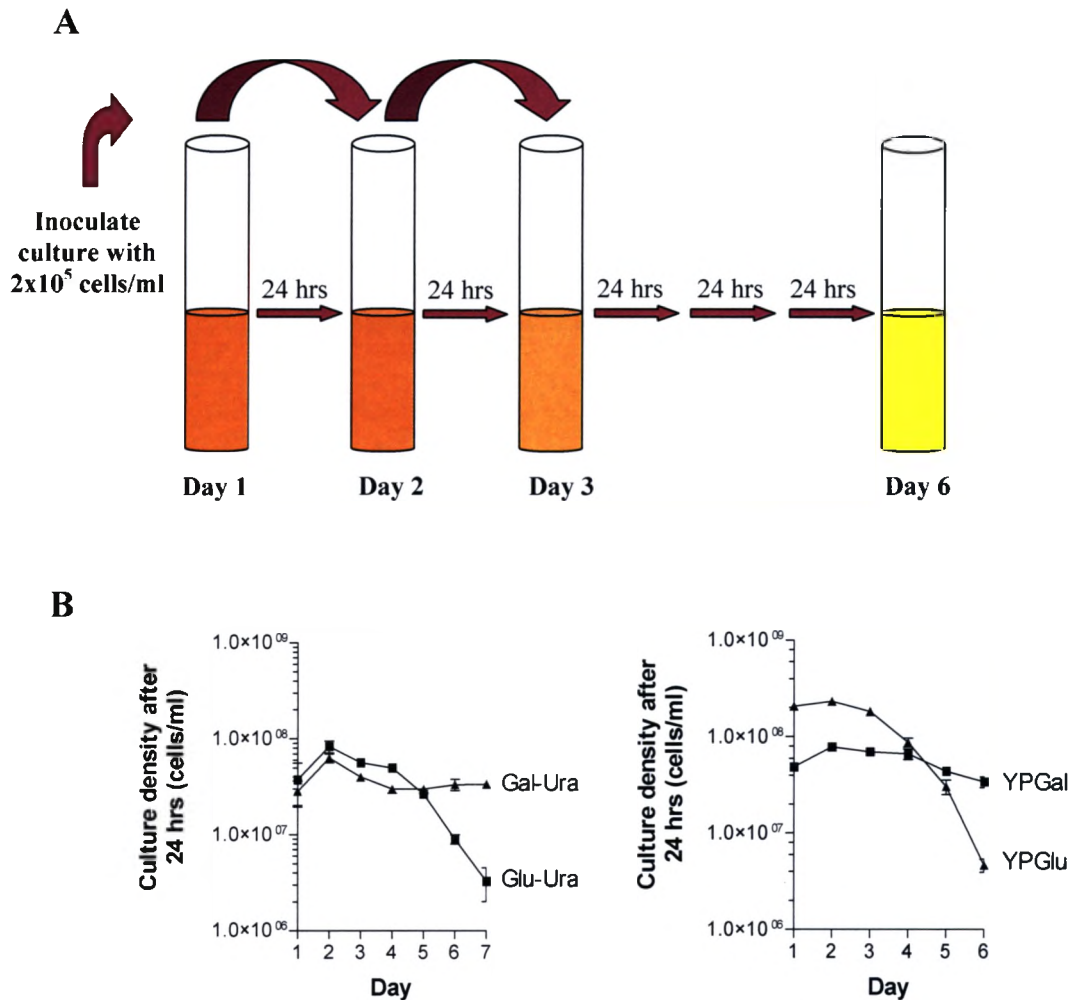


Figure 8. (A) Schematic representation of the liquid growth culture assay. A low titer of cells was inoculated into fresh growth media after 24 hours. (B) Growth curves reflecting the cell titers measured microscopically after 24 hrs grown in synthetic media (Glu-Ura and Gal-Ura) or rich media (YPGlu and YPGal).

The previous tests monitored growth potential of cells in liquid media. The colony forming ability of cells was also tested by measuring plating efficiency, which is defined as the number of cells able to form colonies on plates divided by the number of cells in the culture counted microscopically. As shown in Figure 9, the percentage of cells that were viable, i.e. able to form new colonies on plates, decreased sharply after 4-6 days in

culture. Late passage cultures (after day six) showed an increase in the amount of viable cells, due to the accumulation of “survivor” cells. Studies carried out by Le et al. concluded that these atypical cells are mutants that have increased levels of rearrangements that amplify their telomeric regions, which results in the generation of stable telomere ends (3). These cells achieve such stability via increased Rad52-mediated homologous recombination among telomeres (3). *est2⁻ rad52⁻* double mutants did not form survivors (3; this work). Furthermore, a slower growth rate was observed in cultures passaged after day 4 (~ 50 generations) coinciding with an increase in the amount of dead cells (Figure 8B and 9).

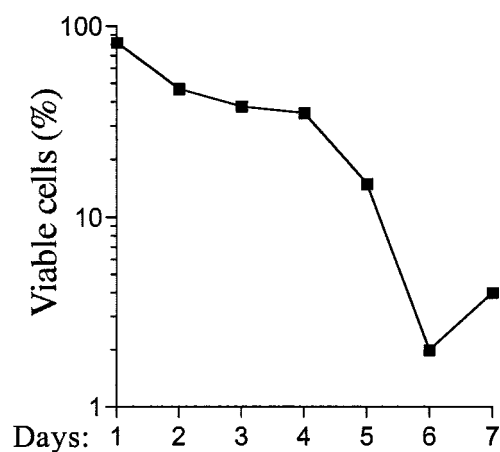


Figure 9. Percent viable cells (plating efficiency) to measure colony forming ability of cells.

Plating efficiency was determined as the number of cells able to form colonies on plates divided by the number of cells measured microscopically

In telomerase-inactivated yeast cells, progressive shortening of telomeres is accompanied with loss in growth potential, increased chromosome instability and cell death. As telomeres get progressively shorter the chromosome ends are thought to become “uncapped” and resemble double-strand breaks (DSBs) and therefore trigger

DNA damage response mechanisms. The process is similar to exposing cells to ionizing radiation (X-rays, etc.) or other DNA damage inducing agents that cause the accumulation of DSBs. These treatments instigate cells to enter a G_2 -phase cell cycle arrest (Figure 10) until the damage has been repaired (2, 42, 43, 44).

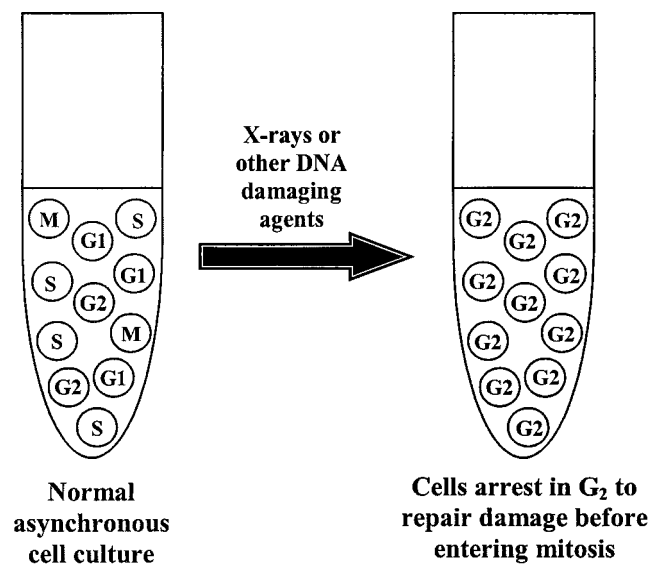


Figure 10. Illustration of the impact on cells when they are subjected to X-rays or other DNA damaging agents.

As senescing yeast cells lose telomeric DNA sequences and enter G_2 arrest they become greatly enlarged indicating stress and perhaps continued metabolic growth (2). In cells containing the *GAL1-V10::EST2* expression system, G_2 -arrested cells became prominent after the fourth day, i.e., after 40-50 generations. A field of late senescence cells is shown in Figure 11.

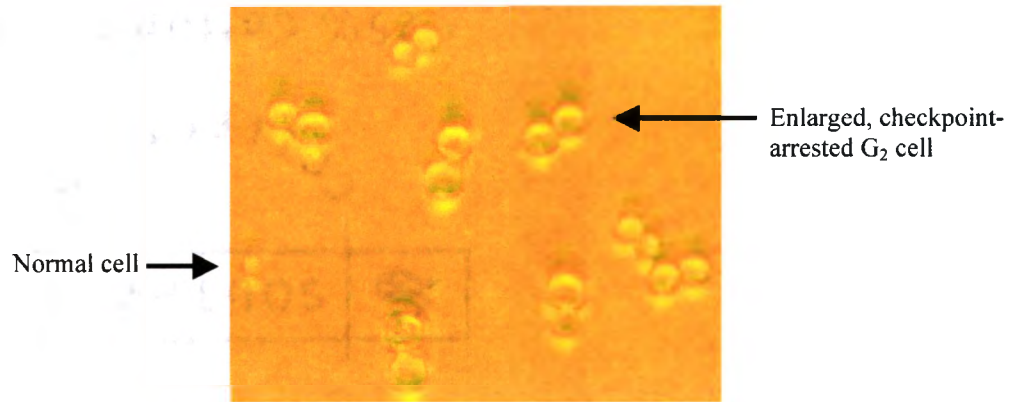


Figure 11. Enlarged senescent yeast cells at the G₂ checkpoint stage after six days of continuous culture imaged using phase contrast light microscopy.

Cell cycle stages in yeast can be quantitated as shown in Figure 12. Unbudded cells are classified as being in G₁ phase, cells with small buds are in S phase, and cells with large buds are termed as being in G₂ or M phase (though most such cells are in G₂).

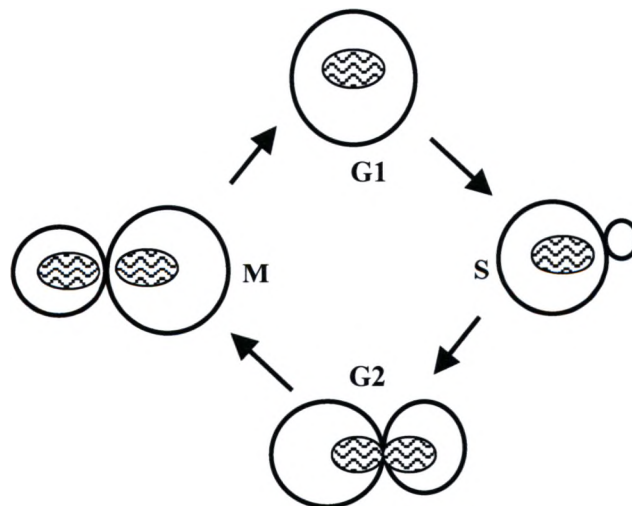


Figure 12. Schematic diagram of budding yeast cells during the stages of the cell cycle.

To quantitate cell cycle effects, *est2*⁻ mutant cells that were passaged continuously in glucose and galactose media were analyzed microscopically every 24 hours. As seen in Figure 13, G₂/M-arrested cells sharply increased in glucose media (*EST2* not expressed) after day four to approximately 70% of all cells. In contrast, cells that were cultured in galactose media showed no significant increase.

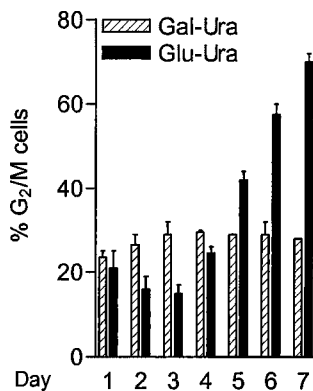


Figure 13. Quantitation of cell cycle arrest of telomerase-deficient yeast cells grown in synthetic media (Gal-Ura and Glu-Ura).

Having established the system, the next set of experiments were designed to address the following: (i) quantitatively assess the events that occur in senescence, and (ii) begin preliminary testing of the major model for senescence in yeast and human cells. The major model proposes that formation of end-to-end fusions (and other possible chromosome rearrangements) is ultimately lethal to senescing cells. Chromosome fusions such as these lead to the establishment of dicentric chromosomes, which have been cited as being the likely cause of cell death (2, 38, 39, 40, 41). Dicentric chromosomes result in increased amounts of rearrangements and deletions due to the two centromeres being pulled apart during mitosis. This brings about the formation of “bridge” structures, which

get sheared creating double-strand breaks and deletion derivatives that have lost one of the centromeres (45, 46).

The next series of senescence assays were optimized based on experience obtained with the preliminary studies. For the next experiments the following improvements were made: (i) the amount of sugar was increased from 3% to 5% (4% for the experiment with bleomycin) to ensure that glucose concentrations remained high, (ii) each culture was inoculated with cells from an independent individual colony instead of from a patch of cells for all cultures to minimize the likelihood of cultures with “survivor” mutants, and (iii) the number of replicates carried out for each culture was increased from 2 to between 4 and 7 to obtain better statistics.

Analysis of growth potential and cell cycle arrest of *est2*⁻ cells under optimized conditions

A liquid growth assay of *est2*⁻ cells was performed where cells were passaged every day in 5% Glu-Ura media for 8 days where they grew up to 9-10 generations every 24 hours and displayed senescence (decrease in cell titers) beginning on days 5 and 6 (~50-60 generations) (Figure 14A). Numbers of G₂/M-arrested *est2*⁻ cells were quantitated every 24 hours during this liquid growth assay where cells were passaged continuously in rich 5% YP glucose or galactose media (Figure 14B). An increase in G₂/M-arrested cells was observed as early as day 4 in YPGlu (*EST2* not expressed) while the levels in YPGal (*EST2* expressed) remained at a consistent level throughout (the slight increase on day 6 was not significant, as the error bars overlapped with those of day 5) (Figure 14B).

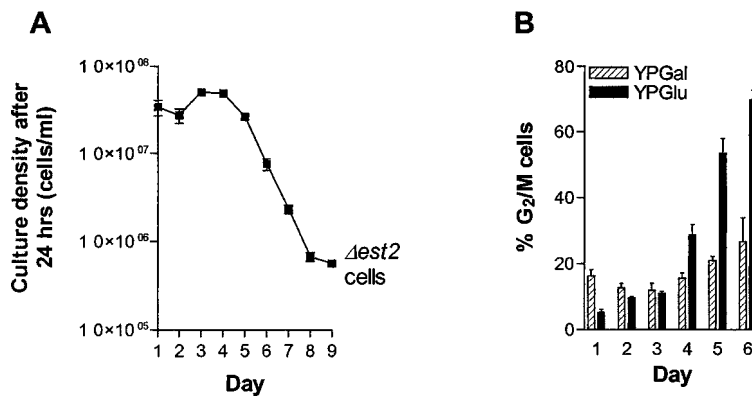


Figure 14. (A) Cell densities of $est2^-$ cells passaged daily in 5% Glu-Ura media. (B) Analysis of G₂/M-arrested $est2^-$ cells grown in galactose or glucose media.

Analysis of growth potential and cell cycling of $est2^- rad52^-$ double mutant cells

To overcome the formation of survivor cells within cultures that arise due to mutants with increased levels of Rad52-mediated homologous recombination, an $est2^- rad52^-$ double mutant strain was created. The chromosomal *RAD52* gene was disrupted via homologous recombination with the G418 resistance gene (*G418^r*). These cells also contained the pLKL82Y plasmid with the *GAL1-V10p::EST2* fusion where the only source of *EST2* was from the plasmid.

After the optimal conditions for the assays with $est2^-$ cells were established, liquid growth density assays were carried out using the $est2^- rad52^-$ double mutant cells. These cell cultures were passaged in glucose media for seven days where an early decrease in the cell titers after day 3 was observed (Figure 15A). $est2^-$ single mutant culture densities did not decrease until day 4 under these conditions (Figure 14A).

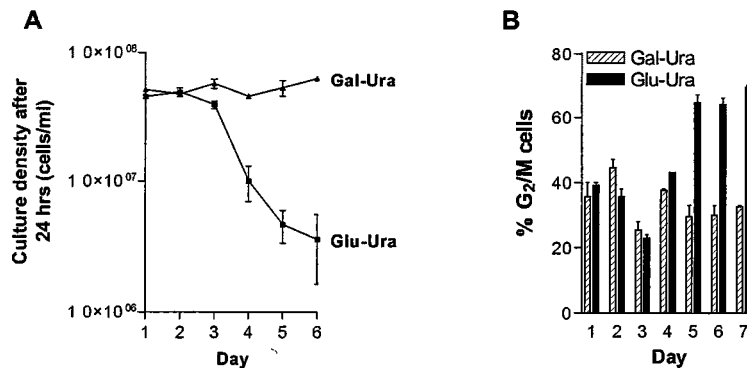


Figure 15. (A) Cell densities of *est2⁻ rad52⁻* cells passaged daily in 5% Glu-Ura media (B) Analysis of G₂/M-arrested *est2⁻ rad52⁻* cells grown in galactose or glucose media.

G₂/M-arrested cells of *est2⁻ rad52⁻* double mutants that were passaged continuously in synthetic glucose and galactose media were also quantitated every 24 hours (Figure 15B). An increase in arrested cells was observed in the double mutants grown in glucose media (*EST2* not expressed) overall beginning after day three (Figure 15B) while increased G₂/M cells for the single mutants were not prominent until after day four (Figure 14B). The percentage of G₂/M-arrested cells was clearly higher in the *est2⁻ rad52⁻* double mutant on days 4, 5 and 6 (during late senescence). Neither of the strains exhibited cell cycle arrest when grown in galactose media (Figure 14B and 15B).

Testing senescence models: does reactivation of telomerase in late senescence rescue cells that would otherwise die?

In order to investigate, for the first time, the reversibility of senescence, the quantity of viable cells present at every 24 hour time point was calculated by spreading appropriate dilutions on either rich (YPGlu and YPGal) or synthetic (Glu-Ura and Gal-Ura) plates. The major question that was addressed was whether late senescent cells at

the threshold of death in late senescence can be rescued by reactivation of telomerase expression. This was accomplished by spreading cells onto galactose plates to turn on the *GAL1-V10p::EST2* fusion.

These assays were carried out with *est2⁻* cells (Figure 16) and *est2⁻ rad52⁻* cells (Figure 17) grown in 5% glucose media and spread onto nonselective YP or selective synthetic galactose and glucose plates. The number of rescued cells on galactose vs. glucose plates was calculated by taking the ratio of the number of colonies on galactose plates to the number of colonies grown on glucose plates and shown in the figures as Gal to Glu ratios.

A gradual loss in viability (i.e., the number of cells able to form colonies) was observed in *est2⁻* cells spread to all plates during the time-course. However, there was a considerable increase in the number of cells that were rescued (Gal vs. Glu) when *EST2* was turned back on. This was true using both rich YP media (Figure 16A) and on synthetic media (Figure 16B), which selects for plasmid-containing cells. The lower overall numbers on –Ura plates than on non-selective YP plates suggests that a significant fraction of cells had experienced plasmid loss. This is consistent with the known increase in chromosome instability during senescence. Importantly, late senescence cells (days 5-8) showed an increase of 2-fold to 6-fold in the fraction of cells that formed colonies when *EST2* was reactivated.

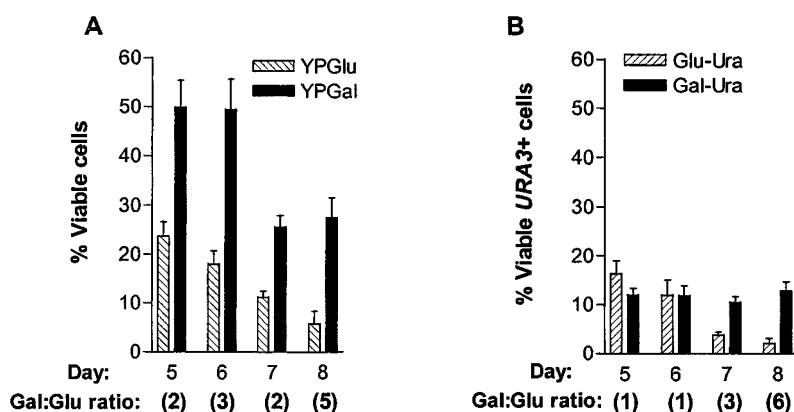
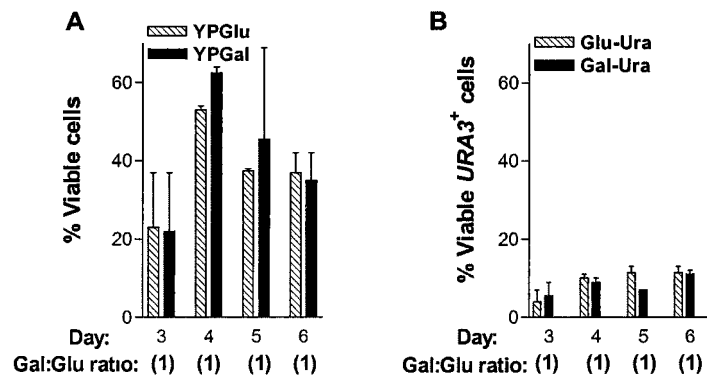


Figure 16. The number of viable cells (%) present in *est2⁻* cell cultures grown daily in liquid glucose for eight days and spread onto (A) YPGlu and YPGal plates and (B) Glu-Ura and Gal-Ura plates

Recombination-deficient *rad52⁻* cells are less able to repair dicentric and other rearranged chromosomes than *RAD52⁺* cells (45). The impact of telomerase reactivation on *est2⁻* cells that were also *rad52⁻* were tested next. Non-senescent *est2⁻rad52⁻* cells grown in 5% galactose media (*EST2* expressed) showed no senescence and no difference in the cells rescued on galactose vs. glucose plates (Figure 117A and 17B).

Growth in Gal-Ura liquid:



Growth in Glu-Ura liquid:

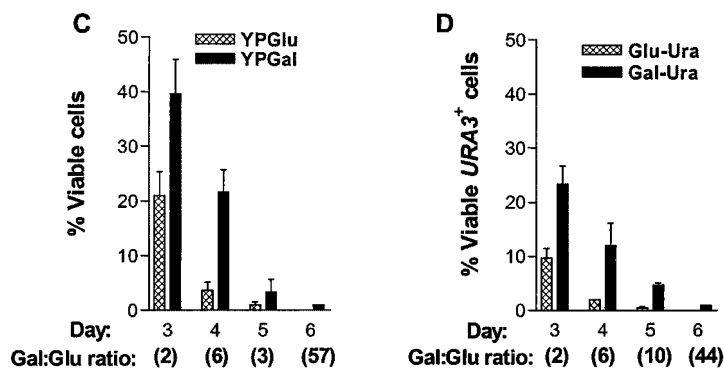


Figure 17. The number of viable cells (%) present in *est2⁻ rad52⁻* cell cultures grown daily in galactose for six days and spread onto (A) YPGlu and YPGal plates or (B) Glu-Ura and Gal-Ura plates. The number of viable cells (%) present in *est2⁻ rad52⁻* cell cultures grown daily in glucose and spread onto (C) YPGlu and YPGal plates or (D) Glu-Ura and Gal-Ura plates.

The efficiency of rescue of senescing *est2⁻ rad52⁻* cells grown in 5% glucose (*EST2* not expressed) was assessed in Figure 17 (C and D). There was an approximately 50 fold difference in the number of rescued *est2⁻ rad52⁻* cells on galactose vs. glucose plates on the 6th day of senescence. For example, on day 6 in Figure 17C, 0.02% of the cells in the culture could form colonies on glucose, but 1% of the cells formed colonies on galactose plates. Thus, the vast majority of cells destined to die after the 6th day (i.e., they could not form colonies when spread onto glucose plates) could be saved by reactivating telomerase (spreading onto galactose plates). This high fraction of rescued

cells was observed using either selective or non-selective plate media (Figure 17C vs. 17D).

In addition to the experiments described above, a different approach for quantitation of the number of viable cells during the late senescence stage of *est2⁻* cells was conducted. *est2⁻* cells were streaked onto Glu-Ura plates as before until the third streak was complete. Seven colonies from these 3rd streaks, which have grown for > 50 generations and would not form colonies if streaked to a 4th plate, were harvested into water and their cell titers calculated. Next, appropriate dilutions of each sample were spread onto synthetic Gal-Ura and Glu-Ura plates. The colonies appearing on the Glu-Ura plates, which included some tiny, near-senescent colonies, were then replica-plated onto fresh Glu-Ura plates and incubated again for 3 days. The colonies that formed were counted and their viable cell titers were calculated. Plating efficiencies were determined as the average titer of cells able to form colonies on the plates divided by the average titer of cells counted microscopically. The results from this experiment demonstrated that there was an approximately 200 fold rescue of late senescing cells when telomerase was turned back on compared to cells that remained telomerase deficient (Table 1). Furthermore, approximately half (41%) of the *est2⁻* cells destined to die could be rescued by reactivation of telomerase. This high number is within 2-fold of the plating efficiency of normal *EST2⁺* cells (70%; Table 1). Thus, both liquid-based and plate-based rescue experiments demonstrated that most cells in late senescence can recover if telomerase is reactivated. These observations suggest that the cells, which have experienced extensive telomere shortening and high chromosome instability, have not formed lethal chromosome rearrangements or lost essential genes from their genomes.

Table 1. Rescue of late senescence *est2*⁻ cells grown on plate media.

Plating Efficiency ^a			
BY4742	<i>est2</i> ⁻ cells		
	Glu	Gal	Gal/Glu
70%	0.2% (±0.1%)	41% (±31%)	227 fold

^a Number of cells able to form colonies on plates divided by number of cells counted microscopically (± standard deviations)

Analysis of biochemical factors that influence the rate of *in vitro* cell aging

Although the primary cause of replicative senescence is telomere shortening caused by the lack of telomerase, the rate of shortening can vary among humans (6). Recent studies have suggested that DNA damage, especially oxidation, may influence the rate of cell aging *in vivo* and in cell culture (13, 14, 16, 17). Having established the phenotypes of normal senescence, the next experiments were designed to evaluate the influence of oxidative DNA damage and other types of DNA lesions on the process. The pro-oxidants used for these experiments were bleomycin and hydrogen peroxide. Bleomycin is a DNA single- and double-strand break inducing agent that binds iron and oxygen to form a free radical complex (18, 19, 20). Hydrogen peroxide generates peroxy and hydroxyl radicals that cause oxidative damage to biomolecules within cells. The influence of antioxidants (N-acetylcysteine and resveratrol) was also tested to determine their influence on *in vitro* cell aging.

Analysis of growth potential and cell cycling of *est2*⁻ cells in the presence of the pro-oxidant bleomycin

Liquid growth culture assays were performed with *est2*⁻ cells in galactose (*EST2* expressed) and glucose media (*EST2* not expressed) containing a sub-lethal dose of 0.1 µg/ml bleomycin. Daily cell densities were measured and the number of G₂/M arrested cells present at every 24 hour time point was quantitated microscopically (Figure 18). Non-senescent cells grown in galactose plus bleomycin maintained a consistent cell density throughout (Figure 18A) and the concentration of bleomycin used slowed the growth rate of cells slightly, but did not cause loss of growth capability or cell death. In contrast, cells grown in glucose demonstrated a steady decrease in cell densities after day 2 (Figure 18B). Interestingly, this non-lethal dose of bleomycin caused an apparent acceleration of the senescence process in the *est2*⁻ cells grown in glucose (Figure 18B).

Cell cycle-arrested cells were also quantitated microscopically every 24 hours. Cells grown in glucose plus bleomycin displayed a moderate increase in G₂/M cells during most of senescence, especially days 3, 4, and 5 compared to cells that were grown in glucose alone (Figure 18D). Cells grown in galactose (non-senescent cells) did not show arrest and the number of G₂/M cells was only slightly increased when bleomycin was included in the media (remaining at ~20-30% throughout the time-course) (Figure 18C). Thus, in the presence of bleomycin, culture densities were unchanged in galactose (during 6 days), but cells stopped growing and arrested in G₂ with accelerated kinetics in glucose.

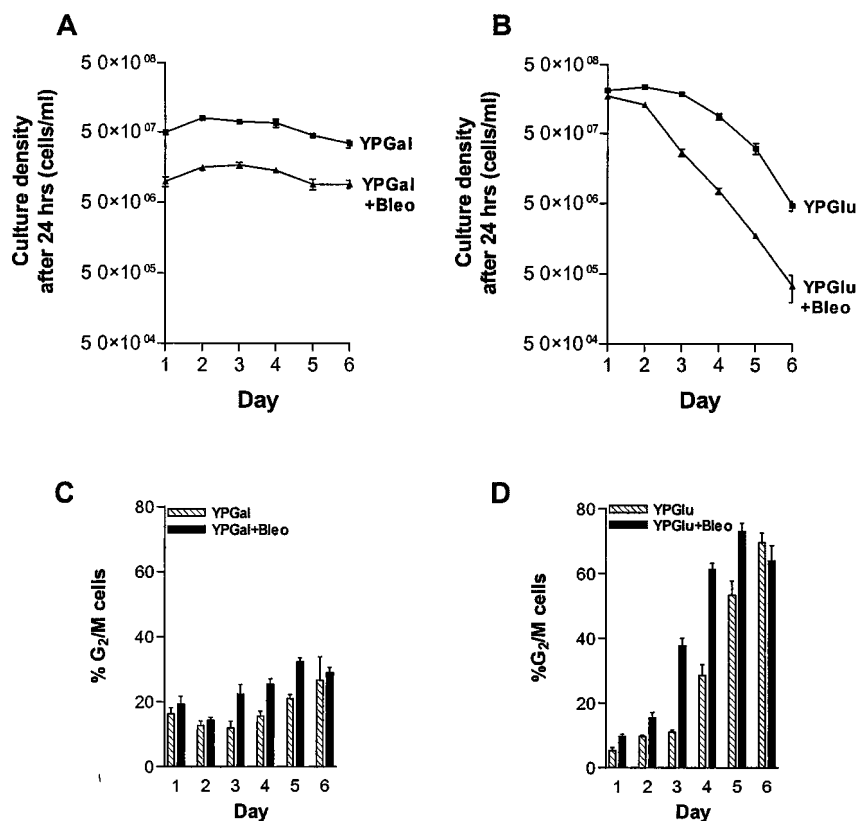


Figure 18. Experiments with *est2⁻* mutant cells and $\pm 0.1 \mu\text{g/ml}$ bleomycin. (A) Growth curves reflecting the cell titers measured microscopically after 24 hrs grown in 4% galactose (YPGal). (B) Growth curves after 24 hrs grown in 4% glucose (YPGlu). (C) Quantitation of G₂/M cells in galactose in the presence and absence of bleomycin. (D) Quantitation of G₂/M cells in glucose in the presence and absence of bleomycin

This sub-lethal dose of $0.1 \mu\text{g/ml}$ bleomycin demonstrated modest growth inhibition of cells, but no killing effect. As depicted in Figure 18A, bleomycin cultures grew throughout the time-course, but did not quite reach the high densities of cells in galactose media without bleomycin. Therefore, the same experiment was carried out using a lower dose of $0.05 \mu\text{g/ml}$ bleomycin to observe if accelerated senescence still occurred without demonstrating a growth inhibition effect (Figure 19).

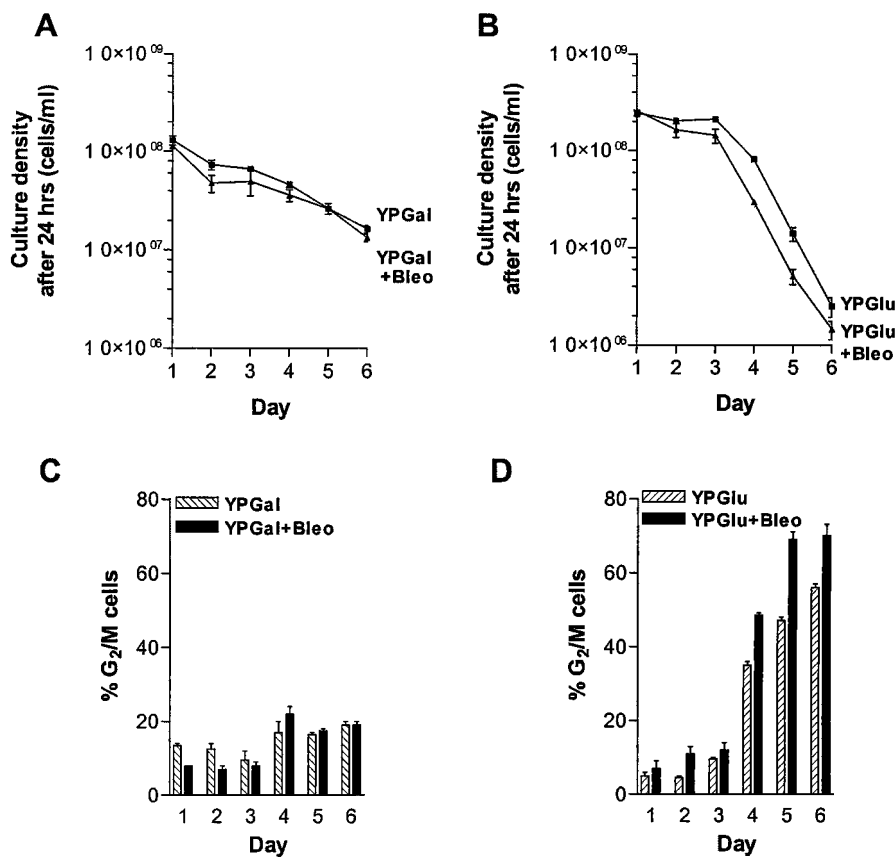


Figure 19. Experiments with *est2⁻* mutant cells and $\pm 0.05 \mu\text{g/ml}$ bleomycin. (A) Growth curves reflecting the cell titers measured microscopically after 24 hrs grown in 4% galactose (YPGal). (B) Growth curves after 24 hrs grown in 4% glucose (YPGlu). (C) Quantitation of G₂/M cells in galactose in the presence and absence of bleomycin. (D) Quantitation of G₂/M cells in glucose in the presence and absence of bleomycin

Cells grown in galactose plus $0.05 \mu\text{g/ml}$ bleomycin (the lower dose) showed no difference in growth rate from cells grown in galactose alone (Figure 19A). Furthermore, cells grown in glucose plus bleomycin again showed a modestly increased rate of senescence, though the effect was less than before (Figure 19B).

The lower dose of bleomycin had no effect on cycling of cells grown in galactose (*EST2⁺*) (Figure 19C). In contrast, G₂/M cell counts showed that more cells accumulated damage and arrested in the G₂/M phase in glucose plus bleomycin than cells grown in the

absence of bleomycin throughout late senescence (days 4, 5, and 6) (Figure 19D). These numbers were significantly higher than mutant cells grown in glucose minus bleomycin.

Analysis of growth potential of *est2*⁻ and *est2*⁻ *rad52*⁻ cells in the presence of bleomycin via plate assays

In addition to the liquid media bleomycin tests, senescence was also tested using plate assays at concentrations of 0.1 µg/ml and 0.5 µg/ml bleomycin. Plate assays were performed using *est2*⁻ and *est2*⁻ *rad52*⁻ cells from a galactose plate (*EST2* expressed) and streaked onto Glu-Ura and Gal-Ura plates, incubated for 3 days and restreaked. As seen in Figure 20, senescence in *est2*⁻ cells streaked on glucose media (*EST2* not expressed) with no bleomycin added, was observed on the 4th streak (Figure 20A-right side), while senescence in *est2*⁻ *rad52*⁻ cells on plates with no bleomycin was observed on the 3rd streak (Figure 20B-right side). Thus, the plate assays were capable of reproducing the accelerated senescence phenotype of *rad52*⁻ cells that was seen in liquid cultures.

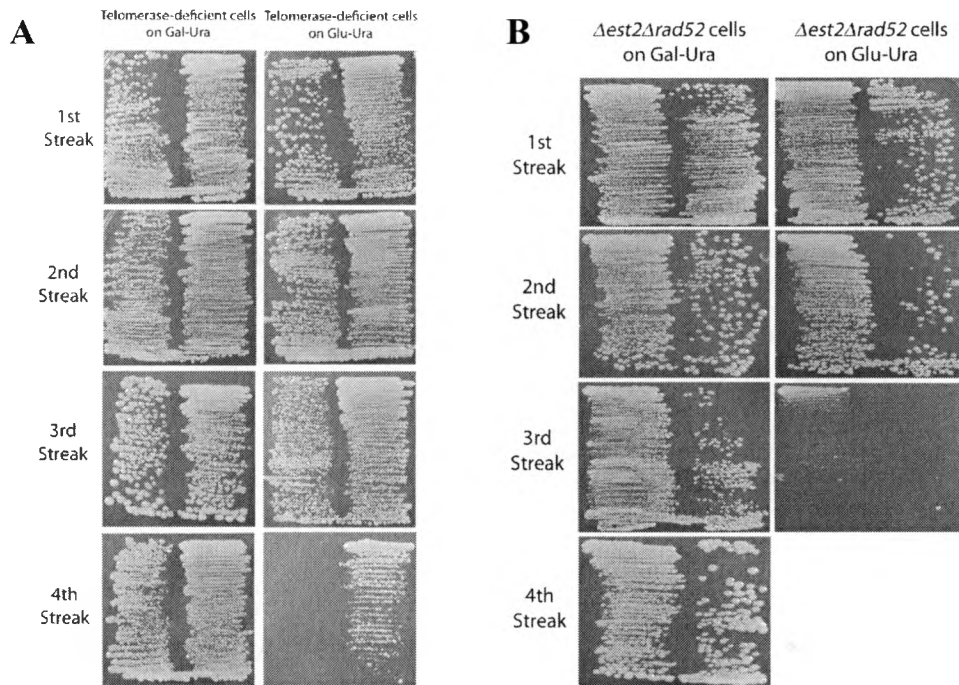


Figure 20. (A) *est2⁻* cells grown on Gal-Ura (*EST2* expressed) and Glu-Ura (*EST2* not expressed) plates with no bleomycin. (B) *est2⁻ rad52⁻* cells grown on Gal-Ura (*EST2* expressed) and Glu-Ura (*EST2* not expressed) plates with no bleomycin.

Streak tests on glucose plus 0.5 $\mu\text{g/ml}$ bleomycin were carried out using *est2⁻* and *est2⁻ rad52⁻* cells (Figure 21). Each of these cells was streaked onto Glu-Ura plates containing bleomycin from individual colonies as seen in Figure 20. Wildtype BY4742 cells (*EST2⁺*) were also streaked on glucose-complete plates containing bleomycin as a control. The wildtype streaks done with either 0.1 $\mu\text{g/ml}$ or 0.5 $\mu\text{g/ml}$ bleomycin did not show any effect on cell growth (Figure 21-left side and data not shown). Bleomycin showed only a slight effect on senescence, with colony sizes in *est2⁻* cells on the 3rd streaks consistently smaller than those formed in the absence of bleomycin (Figure 21-middle column). Streaks for *est2⁻ rad52⁻* cells in the presence of bleomycin did not show strong effects on the number of visible colonies, but colony sizes and apparent growth rates were generally moderately decreased (Figures 20 and 21 – 2nd streaks).

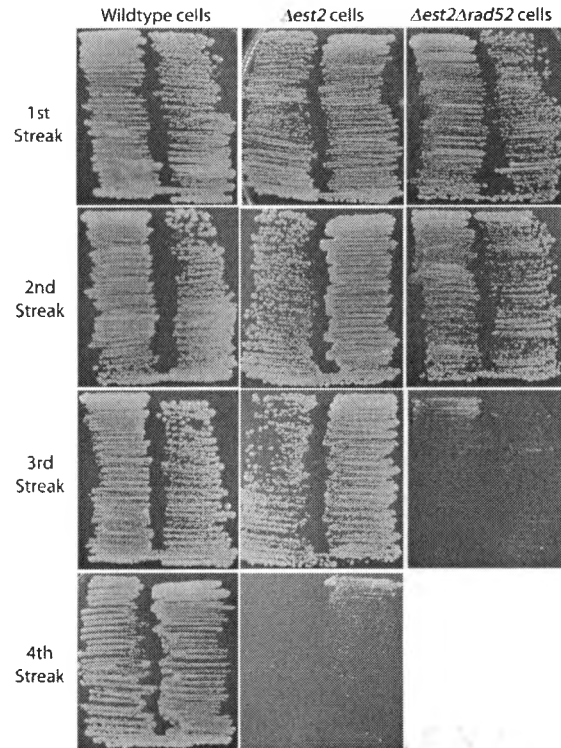


Figure 21. *est2⁻* and *est2⁻ rad52⁻* cells grown on Glu-Ura plus 0.5 $\mu\text{g/ml}$ bleomycin. The mutant cells did not show any change in senescence pattern with the dose of bleomycin used.

Preliminary analysis of the impact of other well-characterized pro- and antioxidants on *in vitro* cell aging

Liquid culture growth assays carried out with *est2⁻* cells in the presence of 0.5 mM, 0.1 mM or 0.25 mM hydrogen peroxide in glucose revealed no strong effect on senescence (data not shown). Higher doses of H_2O_2 as well as another peroxide, tert-butyl hydroperoxide, are currently being investigated in the lab. The antioxidants N-acetylcysteine and resveratrol were used to assess their impact on cell senescence. Resveratrol, an antioxidant found in grapes, berries and peanuts, aids in the prevention of particular vascular diseases and cancer (47, 48). Evidence suggests that the antioxidant

N-acetylcysteine has effects in reducing oxidative stress related to renal failure (49). Liquid culture growth assays carried out with *est2⁻* cells and 20 mM N-acetylcysteine, 40 mM N-acetylcysteine and 0.1 mM resveratrol in glucose as done in the previous assays, showed no effect on senescence (data not shown). Future work on this project will test higher doses in normal cells and in mutant cells that are defective in the neutralization of oxygen-derived free radicals.

Preliminary analysis of senescence in *est2⁻/est2⁻* diploid cells

After establishing a successful system in haploid yeast cells, further experiments were performed to assess the possibility of carrying out similar experiments using diploid cells, which are more like human somatic cells. It is possible to mate haploid yeast cells of opposite mating type to form diploids. In an attempt to analyze details of senescence in diploid yeast cells, BY4742 cells lacking *EST2* were mated with *est2⁻* cells of another strain called YB146 to produce *est2⁻/est2⁻* diploids. The new diploid cells also contained the *GAL1-V10p::EST2* plasmid pLKL82Y (Chapter 2).

Liquid growth potential assays and streak assays were performed using *est2⁻/est2⁻* diploid cells in order to observe the phenotypes and kinetics of senescence. The cells were grown in glucose liquid for more than 8 days and failed to show any signs of senescence (not shown). The same result was seen in streak plate assays: eight consecutive streaks were done on both synthetic and rich glucose media but senescence did not occur. The strains were constructed a second time using an alternative method and still did not show senescence. At present, it is unclear why the cells did not senesce. Future experiments will attempt to resolve this finding, probably by utilizing other lab

yeast strains. The Lewis lab will undertake future experiments using diploid strains and do similar tests as done here with haploid cells.

Summary

In summary, this research project has successfully created and characterized a new system for manipulating cell senescence by the specific control of the expression of telomerase. This was accomplished by placing the yeast *EST2* gene (the catalytic subunit of the telomerase complex) under the control of the specialized galactose-inducible *GAL1-V10* promoter. Mutant cells, which have their chromosomal copy of *EST2* inactivated and contain the *GAL1-V10::EST2* fusion, were unable to synthesize telomerase when grown in glucose media and underwent senescence in both liquid and plate-based assays.

Telomerase is inactivated in human somatic cells after differentiation and telomeres get progressively shorter as DNA is replicated giving rise to chromosome instability brought about primarily by the loss of the telomere-associated proteins (uncapping). The formation of aberrant structures, such as end-to-end fusions and their breakage products, have been cited as the likely cause of cell death in higher eukaryotes and yeast (2, 38, 39, 40, 41). This research project demonstrated that most cells even at the threshold of apparent death can be rescued by turning telomerase (*EST2*) back on, arguing strongly that they had not formed lethal rearrangements during that time.

Fifteen percent of the genes within the yeast genome are essential. Some of these genes are found near the ends of chromosomes. If the main cause of death in cells was the degradation of chromosome ends that eventually led to the inactivation (deletion) of these

essential genes, then the reactivation of telomerase could not have rescued the cells.

Thus, the results of these reactivation experiments argue against two possible models for the loss of viability during senescence: the formation of lethal chromosome rearrangements or formation of terminal deletions that result in the deletion of essential genes.

The exact cause of loss of viability in yeast cells remains unknown. The results of this project suggest a possible model where cells are chronically arrested in the cell cycle, but they do not actually die. According to this model, G₂ checkpoint-arrested senescent cells activate DNA damage responses and are not dead, but have merely lost their ability to grow (divide). When telomerase is turned back on in the senescing cells, the shortened telomeres that were being recognized as broken ends are extended and recapped by recruiting the telomere-associated proteins. Therefore, these chromosomes no longer act as signals for cell cycle arrest in G₂.

Previous studies have suggested that many factors including pro-oxidants may affect *in vitro* cell aging. The data in this study demonstrates that low doses of the pro-oxidant chemical bleomycin that are not lethal to normal cells (or to *est2⁻* cells in early senescence) can accelerate the loss of growth potential that occurs during normal senescence. This agent is a widely studied anti-tumor drug that forms a highly reactive oxygen-iron free radical complex inside cells (18, 19, 20). A past study has suggested that the repeat sequences (especially guanine bases) in telomeres may be especially susceptible to oxidative damage (15, 16, 17). Future experiments will analyze the possibility that bleomycin may accelerate cell senescence by increasing the rate of telomere shortening.

In conclusion, this project was successful in establishing a system in which *in vitro* cell aging can be monitored quantitatively that will be of value for numerous studies in the future. The finding that reactivating telomerase rescues cells from death contradicts previous theories of how cell death occurs, but also suggests new directions for future research on the mechanism of replicative cell senescence.

REFERENCES

1. Epel, E.S.; Blackburn, E.H.; Lin, J.; Dhabhar, F.S.; Adler, N.E.; Morrow, J.D.; Cawthon, R.M. *Proc Natl Acad Sci.* **2004**, *49*, 17312-17315.
2. Ijpmma, A.S.; Greider, C.W. *Mol Biol Cell.* **2003**, *14*, 987-1001.
3. Le, S.; Moore, J.K.; Haber, J.E.; Greider, C.W. *Genetics.* **1999**, *152*, 143-152.
4. Hahn, W.C.; Meyerson, M. *Ann Med.* **2001**, *33*, 123-129.
5. Meeker, A.K., Hicks, L.J.; Platz, E.A.; March, G.E.; Bennett, C.J.; Delannoy, M.J.; de Marzo, A.M. *Cancer Res.* **2002**, *62*, 6405-9.
6. Cawthon, R.M.; Smith, K.R.; O'Brien, E.; Sivatchenko, A.; Kerber, R.A. *Lancet.* **2003**, *361*, 393-395.
7. Vulliamy, T.; Marrone, A.; Goldman, F.; Dearlove, A.; Bessler, M.; Mason, P.J.; Dokal, I. *Nature.* **2001**, *413*, 432-5.
8. Rowley, P.T.; Tabler, M. *Anticancer Res.* **2000**, *20*, 4419-4429.
9. Mondello, C.; Scovassi, A.I. *Biochem Cell Biol.* **2004**, *82*, 498-507.
10. Mukherjee, A.B.; Costello, C. *Mech Ageing Dev.* **1998**, *103*, 209-22.
11. Wong, K.K.; Chang, S.; Weiler, S.R.; Ganesan, S.; Chaudhuri, J.; Zhu, C.; Artandi, S.E.; Rudolph, K.L.; Gottlieb, G.J.; Chin, L.F.; Alt, W.; DePinho, R.A. *Nat Genet.* **2000**, *26*, 85-8.
12. Lundblad, V. *Oncogene.* **2002**, *21*, 522-531.
13. Ames, B.N.; Shigenaga, M.K.; Hagen, T.M. *Proc Natl Acad Sci.* **1993**, *90*, 7915-7922.
14. Beckman, K.B.; Ames, B.N. *Phys Rev.* **1998**, *78*, 547-581.
15. Kaneko, T.; Tahara, S.; Taguchi, T.; Kondo, H. *Mut Res.* **2001**, *487*, 19-30.
16. Oikawa, S.; Kawanishi, S. *FEBS Let.* **1999**, *453*, 365-368.

17. Chen, Q.; Fischer, A.; Yan, L.; Ames, B.N. *Proc Natl Acad Sci.* **1995**, *92*, 4337-4341.
18. Chen, J.; Stubbe, J. *Nat Rev Cancer.* **2005**, *5*, 102-12.
19. Ramotar, D.; Wang, H. *Curr Genet.* **2003**, *43*, 213-24.
20. Sikic, B.I. *Cancer Surv.* **1986**, *5*, 81-91.
21. Melov, S.; Ravenscroft, J.; Malik, S.; Gill, M.S.; Walker, D.W.; Clayton, P.E.; Wallace, D.C.; Malfroy, B.; Doctrow, S.R.; Lithgow, G.J. *Science.* **2000**, *289*, 1567-1569.
22. Tanguy, S.; Boucher, F.; Besse, S.; de Leiris, J. *Cardiovascular Drugs and Therapy.* **1998**, *12*, 355-357.
23. Orr, W.C.; Sohal, R.S. *Science.* **1994**, *263*, 1128-1130.
24. Furumoto, K.; Inoue, E.; Hiyama, E.; Miwa, N. *Life Sci.* **1998**, *63*, 935-948.
25. Sen, S.; Phillis, J.W. *Free Radical Res. Commun.* **1993**, *19*, 255-265.
26. Cova, D.; De, A.L.; Monti, E.; Piccinini, F. *Free Radical Res Commun.* **1992**, *15*, 353-360.
27. Lingner, J.; Hughes, T.R.; Shevchenko, A.; Mann, M.; Lundblad, V.; Cech, T.R. *Science.* **1997**, *276*, 571-567.
28. Lowell, J.E.; Pillus, L. *Cell Mol Life Sci.* **1998**, *54*, 32-49.
29. Lundblad, V. *Mutat Res.* **2000**, *451*, 227-40.
30. Lewis, L.K.; Lobachev, K.; Westmoreland, J.; Karthikeyan, G.; Williamson, K.; Resnick, M.A. *Gene.* **2005**, Submitted.
31. Johnston, M.; Flick, J.S.; Pexton, T. *Molecular and Cellular Biology.* **1994**, *14*, 3834-41.
32. Lohr, D.; Venkov, P.; Zlatanova, J. *FASEB Journal.* **1995**, *9*, 777-787.
33. Sambrook, J.; Russell, D.W. *Molecular Cloning: A Laboratory Manual*; 3rd Ed; Cold Spring Harbor Laboratory Press: Cold Spring Harbor, NY. **2001**.
34. Gietz, R.D.; Schiestl, R.H.; Willems, A.R.; Woods, R.A. *Yeast.* **1995**, *11*, 355-360.
35. Soni, R.; Carmichael, J.P.; Murray, J.R. *Curr Genet.* **1993**, *24*, 455-459.

36. Goldstein, A.L.; McCusker, J.H. *Yeast*. **1999**, *15*, 1541-53.
37. Lewis, L.K.; Kirchner, J.M.; Resnick, M.A. *Mol Cell Biol*. **1998**, *18*, 1891-902.
38. Ducray, C.; Pommier, J.P.; Martins, L.; Boussin, F.D.; Sabatier, L. *Oncogene* **1999**, *18*, 4211-23.
39. Hayflick, L. *Exp Gerontol*. **2003**, *38*, 1231-1241.
40. Hackett, J.A.; Feldser, D.M.; Greider, C.W. *Cell*. **2001**, *106*, 275-286.
41. van Steensel, B.; Smogorzewska, A.; de Lange, T. *Cell*. **1998**, *92*, 401-13.
42. Enomoto, S.; Glowczewski, L.; Berman, J. *Mol Biol Cell*. **2002**, *13*, 2626-38.
43. Gardner, R.; Putnam, C.W.; Weinert, T. *Embo J*. **1999**, *18*, 3173-85.
44. Sandell, L.L.; Zakian, V.A. *Cell*. **1993**, *75*, 729-39.
45. Kramer K.M.; Brock, J.A.; Bloom, K.; Moore, J.K.; Haber, J.E. *Mol Cell Biol*. **1994**, *14*, 1293-1301.
46. Mythreye, K.; Bloom, K.S. *J Cell Biol* **2003**, *160*, 833-43.
47. Aggarwal, B.B.; Bhardwaj, A.; Aggarwal, R.S.; Seeram, N.P.; Shishodia, S.; Takada, Y. *Anticancer Res*. **2004**, *24*, 2783-840.
48. Delmas, D.; Jannin, B.; Latruffe, N. *Mol Nutr Food Res*. **2005**, *49*, 377-95.
49. Luciak, M. *Rocz Akad Med Bialymst*. **2004**, *49*, 157-61.

VITA

Hiranthi Tanuja Thambugala was born in Christchurch, New Zealand, on January 3, 1978, the daughter of Erandathi Nimalka Abeygoonewardena and Anoma Tissa Thambugala. After completing her work at Alethea International School, Dehiwala, Sri Lanka, in 1996, she entered the University of Otago, Dunedin, New Zealand in January 1998 and then the Texas State University-San Marcos, in January 2000. She received the degree of Bachelor of Science from the Texas State University-San Marcos in May 2003. In September 2003, she entered the Graduate College of Texas State University-San Marcos.

Permanent Address: 179/3 Hill Street
Dehiwala
Sri Lanka

This thesis was typed by Hiranthi Tanuja Thambugala.

